

BRANCHING FREQUENCY OF *THALASSIA TESTUDINUM* (BANKS EX
KÖNIG) AS AN ECOLOGICAL INDICATOR IN FLORIDA BAY

Jill C. Paxson

A Thesis Submitted to the
University of North Carolina at Wilmington in Partial Fulfillment
Of the Requirements for the Degree of
Master of Science

Department of Biological Sciences

University of North Carolina at Wilmington

2003

Approved by

Advisory Committee

Courtney T. Hackney

Martin H. Posey

Chair, Michael J. Durako

Accepted by

Dean, Graduate School

TABLE OF CONTENTS

Abstract.....	iii
Acknowledgments.....	v
List of Tables.....	vi
List of Figures.....	vii
INTRODUCTION.....	1
METHODS.....	6
Study Site.....	6
Sampling Design.....	7
Landscape Design.....	9
Bathymetry.....	10
Determination of Light Availability.....	12
Statistics.....	14
RESULTS.....	15
DISCUSSION.....	26
Literature Cited.....	33
Appendix.....	37

Abstract

The effects of short-shoot density and light availability on rhizome apical meristem density and rhizome branch frequency of *Thalassia testudinum* were assessed in ten basins in Florida Bay. Core samples for density measurements were obtained from 27-30 stations per basin (over 300 sampling stations total) during the spring 1998 and spring 1999 sampling of the Fish Habitat Assessment Program (FHAP). Rhizome branch frequency (apicals short-shoots⁻¹) was calculated from the core data. Light attenuation, (K_d), estimated from in situ measurements of secchi depths, light profiles of scalar irradiance and K_d values calculated from AVHRR satellite imagery using GIS indicated high light availability and similar optical water quality between the two years. Light attenuation estimates were coupled with USGS bathymetry to determine if there was a significant interaction between light availability and *Thalassia* densities or rhizome branching.

Apical density and short-shoot density were linearly correlated in Florida Bay. Neither apical density nor rhizome branch frequency in 1998 was found to be a good predictor of short-shoot density fluctuations between the spring of 1998 and 1999. Increases in rhizome branch frequencies were only weakly associated with between-year increases in short-shoot densities in this study. Mean rhizome branch frequencies were 0.19 ± 0.02 , and 0.15 ± 0.01 , for spring 1998 and spring 1999, respectively. The relatively lower rhizome branching rates observed in Florida Bay in 1998 and 1999 may reflect a density-dependent inhibitory response due to the increase in short-shoot densities following the

seagrass die-off from 1990 to 1998 (305 short shoots/m² in 1990, Durako 1995 versus 590 & 602 short shoots/m² in this study).

There was a positive relationship between percent surface irradiance and short-shoot density. In conclusion, rhizome branch frequency was not a good ecoindicator of light availability or short-shoot density changes in Florida Bay. In contrast, it appears that the effect of short-shoot density, which did respond positively to increasing light availability, may be more important in effecting rhizome branching. Therefore, rhizome branch frequency may be a biological indicator that responds to short-shoot density changes in this non-light limited Bay.

Acknowledgments

I would like to extend my great appreciation to my professor for his guidance and patience throughout my research, and to my friends and family for their support during the rough times.

List of Tables

Table		Page
1	Mean (\pm SE) of different variables from t-tests of the spring of 1998 and the spring of 1999.....	17
2	Summary of linear regression analyses for the morphometric relationships between short-shoot density (SSD), apical density (APD), and rhizome branch frequency (BF) or apical density.....	19
3	Summary of multiple or linear regression analyses for the physical relationships between light attenuation (KDR), percent surface irradiance (SI), and short-shoot density (SSD), apical density (APD), or rhizome branch frequency (BF); and linear regression of water depth (USGS) and BF.....	25

List of Figures

Figure		Page
1	Map of Florida Bay with Fish-Habitat Assessment Program study sites illustrating sampling stations as polygons and spring 1998 and spring 1999 GPS station locations marked as point.....	8
2	Flow chart illustrating importation and manipulation of AVHRR, morphometrics, and bathymetric data into GIS for exportation into spreadsheets.....	11
3	Linear regression of light attenuation, K_d , obtained from May 1999 light profile data using quantum sensors (KDP) and AVHRR data from May 1998 (KDR).....	18
4	Linear regression of the square root of apical densities (APD) and the square root of short-shoot densities (SSD) (raw data inset).....	20
5	Linear regression of (a) arcsine square root transformed rhizome branch frequency (BF) and short-shoot density (SSD) – 327 data pts hidden (raw data inset) and (b) linear regression of BF and square root transformed SSD where only apical density and short-shoot density occur together – 155 data pts hidden.....	21
6	Box plot illustrating the mean (dashed line), median (solid line), quartiles, and outliers (dots) of rhizome branch frequency by basin (geographic distance from west to east).....	23
7	Linear regression of rhizome branch frequency (BF) and the differences in short-shoot densities (DEL) from the spring of 1998 and the spring of 1999.....	27
8	Linear regression of (a) spring 1998 short-shoot density (SSD) and %SI (three month average 1998) for stations where % SI < 15 and (b) linear regression of spring 1998 rhizome branch frequency (BF) and % SI for stations where SI < 15% (three month average 1998) (inset excludes 10 cores with short-shoots only).....	28

INTRODUCTION

A biological indicator produces a measurable response that gives a signal of a biological condition. An ecoindicator produces a measurable response that can ultimately give the signal of an ecosystem condition (Linton and Warner 2003). These relationships are critical for establishing baseline data, which can be used as an early warning system that may directly mitigate critical resources

Seagrasses are important primary producers in shallow coastal environments and estuaries (Powell et al. 1989, Short et al. 1991). Their morphology and leaf canopy provide structure for a high diversity and density of associated biota. Seagrass beds provide essential habitats and protection for numerous transient and resident organisms (Heck and Orth 1980, Zieman et al. 1989). Seagrasses are also useful biological indicators (Nichols et al. 1982, Tomasko and Lapointe 1991) and seagrass abundance influences public perception regarding the “health” of coastal ecosystems (Pergent et al. 1999; Orfanidis et al. 2003). Consequently, any change in the distribution or abundance of seagrasses may be perceived as a change in the health of the ecosystem (Linton and Warner 2003).

Thalassia testudinum, Banks ex König (Hydrocharitaceae), turtle grass, is considered to be the climax seagrass species in tropical Caribbean and subtropical Atlantic and Gulf seagrass ecosystems. *Thalassia* beds frequently contain populations of commercially and recreationally important juvenile fish (i.e. red drum, spotted sea trout, snook, and snapper), and invertebrates (i.e. bay scallops, pink shrimp, and blue crabs) (Thayer et al. 1975, Zieman et al. 1989,

Orth and vanMontfrans 1990, Robblee et al. 1991). It is also the dominant marine angiosperm in tropical and subtropical environments (den Hartog 1970, Van Tussenbroek 1996). Loss of this species can have direct effects on the trophic dynamics and structure of the seagrass community (den Hartog 1987, Tomasko et al. 1996).

Turtle grass is a clonal species, with the majority of its growth occurring by vegetative propagation (Tomlinson 1974). The growth pattern of *T. testudinum* is highly organized, showing two distinct axis morphologies (Tomlinson 1974). Long shoots (or rhizomes) grow horizontally, producing long internodes and scale leaves, while short shoots produce short, vertical internodes and foliage leaves. The nodes are the result of the senescence of scale leaves of the rhizome and leaf blades arising from the short-shoot (Brouns 1985).

Branching of rhizomes and short-shoots is precocious and alternate, with the terminal and lateral meristems morphologically identical. Differentiation of the rhizome from the short-shoot occurs approximately 11 to 13 scale-leaf nodes apart (Tomlinson 1974). Thus, a new short-shoot is initiated every 11 to 13 rhizome plastochrones during vegetative growth (Tomlinson 1974). Branching of a short-shoot apex produces new rhizomes (Tomlinson 1974). The rhizome branches to produce short shoots, and new rhizome apices develop exclusively from branching of the short shoots. This new source of short-shoots promotes vegetative spread and lateral coverage of the seagrass bed (Terrados et al. 1997; van Tussenbroek et al. 2000).

The entire length of the monopodial rhizome of *T. testudinum* comprises the genetic individual or genet (den Hartog 1970, Tomlinson 1974, van Tussenbroek 1996). Networks of underground rhizomes are known to produce extensive turtle grass meadows in the Caribbean and Gulf of Mexico (den Hartog 1970, Zieman et al. 1989, van Tussenbroek 1996). Turtle grass rhizomes act as a carbon source (Tomlinson 1974). Carbon is extracted from the water column by way of the green blades and photosynthesis (Phillips and Menez 1988). Due to the lack of photosynthetic tissues in the roots and rhizomes, these structures are dependent upon the carbon production in the photosynthetic leaves. Rhizomes also function as a carbon sink that continuously supports growth and maintenance of the entire genet (Phillips and Menez 1988, Tomasko and Dawes 1988, Tomasko and Dawes 1990, Lee and Dunton 1997, van Tussenbroek et al. 2000). High root/shoot ratios are characteristic of *T. testudinum*'s carbon allocation. The below-ground portion (short-shoot sheaths and rhizome) of turtle grass may account for greater than 80% of the total biomass (Powell et al. 1989, Fourqurean and Zieman 1991, Durako 1995).

The rhizome also contributes to seagrass recovery from physical disturbance (Duarte and Sand-Jensen 1990). The network of rhizomes and short-shoots is produced by rhizome and short-shoot apical meristems, which enable continuous vegetative growth and branching (Tomlinson 1974). Since bed expansion is supported by reallocation of photosynthetic products, there is a direct coupling between the production of short shoots and the production of apical meristem tissues (Duarte and Sand-Jensen 1990). The patterns of

rhizome branching and growth are indicative of the potential for shoot production. Understanding the relationship between rhizome apical densities and short-shoot recruitment may eventually assist in forecasting the recovery of seagrass beds and associated biota following disturbances (Duarte and Sand-Jensen 1990).

Clonal growth of seagrasses is controlled by the apical meristem (Tomlinson 1974, Tomasko et al. 1991, Terrados et al. 1997, van Tussenbroek et al. 2000), which is the source of all vegetatively produced biomass. Since all organs, including the roots and short-shoot meristems are initiated by the terminal meristems, *T. testudinum* is completely meristem dependent (Tomlinson 1974). Meristem-dependent species require a constantly-active shoot-apical meristem for the maintenance of seagrass populations. Gallegos et al. (1993) determined a close dependence of short-shoot density and rhizome biomass on the proliferation of the rhizome. Rhizome apical density and rhizome/short-shoot branching are related to short-shoot density. Thus, growth of apical meristems facilitates turtle grass population maintenance (Tomlinson 1974, Durako 1994, Terrados et al. 1997). Because of the coupling between rhizome growth and branching and short-shoot production, apical density may be a useful ecological indicator for *T. testudinum* reflecting the potential for production and spread (Durako 1995).

Light limitation directly affects productivity, biomass, and carbon allocation patterns in seagrasses (Dennison 1987). Short et al. (1991) suggested that pollution, disease, and increasing human activity increase eutrophication and suspended sediments. These factors, when combined, create low light

conditions that can negatively impact seagrass productivity. Lee and Dunton (1997) reported that *T. testudinum* negatively responds to reductions in irradiance by exhibiting decreased shoot density, growth rate, and biomass. Duarte (1991) suggested that seagrass beds receiving less than 15% of surface irradiance would be light limited. Thus, optical water clarity has become increasingly recognized as the principal limiting factor for the continued maintenance of healthy seagrass meadows (Tomasko and Dawes 1988, Tomasko and Dawes 1989, Fourqurean and Zieman 1991, Onuf 1996). Light availability to the leaves affects photosynthesis, carbon fixation and carbon available for allocation to rhizome apical growth. Light limitation, whether due to increasing depth, turbidity, or, epiphyte cover, will reduce the carbon available for storage within the rhizome network. In addition, disease may limit photosynthesis and carbon fixation capacity of short-shoots (Durako and Kuss 1994). Therefore, rhizome growth, apical density, and rhizome branching should decrease as a function of decreasing light or decreasing photosynthesis.

The objectives of this study were (1) to determine if there is a relationship between shoot density and apical density in *Thalassia testudinum* populations. (2) to determine if there is a relationship between shoot density and rhizome branch frequency. (3) to determine if rhizome branch frequency varies as a function of depth or light availability. (4) to determine if apical density or rhizome branch frequency are predictors of subsequent changes in short-shoot density.

METHODS

Study Site

Florida Bay is a shallow triangular embayment located at the southern tip of the Florida peninsula. It is bounded to the north by the Florida mainland and to the southeast by the Florida Keys; the Gulf of Mexico borders the western margin (Robblee et al. 1991). Salinities in the Bay oscillate between brackish and hypersaline levels. The dominant submerged macrophyte in the portion of Florida Bay within the Everglades National Park boundaries is *T. testudinum*. This area is approximately 1800 km², and greater than 90% of the Bay has turtle grass, while mangroves cover approximately 7% of the Bay (Zieman et al. 1989, Robblee et al. 1991).

A widespread die-off of seagrasses was first observed in Florida Bay in the summer of 1987 (Robblee et al. 1991). Over 4000 ha of seagrasses have been lost since this phenomenon began and another 23,000 ha have been affected. There are many factors thought to have been important in initiating this die-off. These include abnormally high temperatures and salinities, chronic hypoxia of rhizomes, reduced freshwater input and storm frequency, and the outbreak of a disease caused by an undescribed species of the marine slime mold *Labyrinthula* (Robblee et al. 1991, Carlson et al. 1994, Durako 1994, Durako and Kuss 1994). Die-off is characterized by almost total mortality within dense *Thalassia* patches and affects primarily beds located within shallow protected areas (Robblee et al. 1991).

For several years following the onset of the die-off in Florida Bay, the waters remained clear. However, late in 1991, widespread turbidity was first observed. The turbidity, which persisted throughout the mid 1990's, was attributed to phytoplankton blooms and resuspended sediments (Phlips et al. 1995). The more recent losses of seagrasses are more widespread in the deeper turbid basins of western Florida Bay and characterized by "stand thinning" within affected beds, rather than the patchy mortality characteristic of die-off (Durako et al. 2001). It is thought that this secondary mortality has affected seagrass meadows that became light limited because of increasing plankton and sediment resuspension (Phlips et al. 1995, Stumpf et al. 1999).

Sampling Design

Samples used for analysis in this study were collected during the spring 1998 and spring 1999 sampling of the Fisheries Habitat Assessment Program (FHAP). FHAP was initiated in the spring of 1995 in response to the continuing concern regarding the extent of seagrass changes within Florida Bay following the initial die-off in 1987, the subsequent widespread turbidity, and the need to monitor the effects on Florida Bay seagrass communities of water management alterations imposed as part of the restoration of the Everglades/Florida Bay ecosystem (Hall et al. 1999, Durako et al. 2001).

The primary objective of FHAP is to assess the spatial and temporal trends in macrophyte distribution and abundance among ten basins within Florida Bay. The ten basins sampled by FHAP are representative of the wide range of

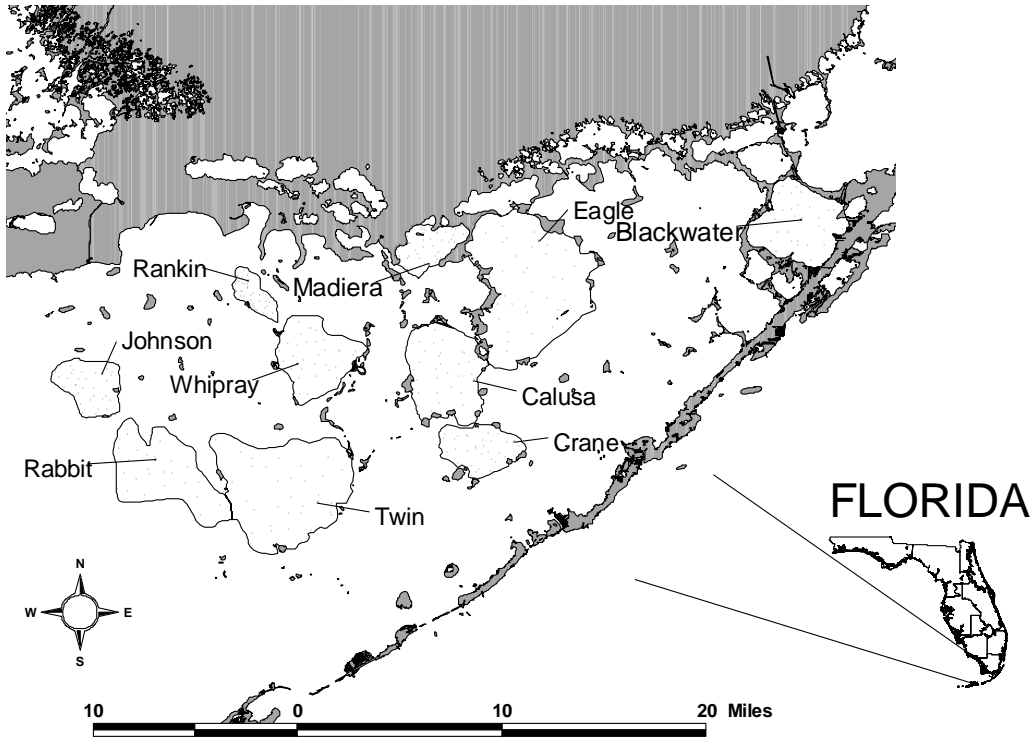


Figure 1
Map of Florida Bay with Fish-Habitat Assessment Program study sites illustrating sampling stations as polygons and spring 1998 and spring 1999 GPS station locations marked as point

conditions within the 1800 km² of the Bay within the Everglades National Park boundaries (Fig. 1). Sampling in FHAP is conducted twice a year in the spring (April/May) and fall (October/November); core samples for quantitative structural and morphometric measurements were obtained during the spring sampling.

Core samples for this study (15-cm diameter, 176.7 cm²) were obtained from each station during FHAP sampling. The numbers of short-shoots and rhizome apicals were recorded for each core. Short-shoot and apical densities were converted to the density per m² by multiplying core values by a constant of 56.6. Rhizome branch frequency was calculated by dividing the number of rhizome apicals by the number of short-shoots per station. Since this research concerned the density and rhizome branching of *T. testudinum*, core samples with no *T. testudinum* were not included in statistical analyses.

Landscape Design

To characterize macrophyte distribution and abundance at the landscape scale required unbiased interpolation across sampling sites. Systematic random sampling within a tessellated hexagonal grid was used to meet these requirements (Fourqurean et al. 2001, Durako et al. 2001). In systematic random sampling, all station points within the landscape have an equal probability of being sampled, and sampling effort is quasi-evenly distributed across the landscape. A random location is chosen as a sample site from within each hexagonal sub-unit. In contrast, complete random sampling points may lead to clumped and non-uniformly distributed data points. Each basin sampled in FHAP

contains approximately 30 stations located within a tessellated hexagonal grid system developed by the USEPA's EMAP program. Site locations were located in the field using Global Positioning Systems (GPS).

To increase our ability to detect changes in *Thalassia testudinum* distribution and abundance, the same sites were sampled during the spring of 1998 and 1999. This allowed for direct comparison of short-shoot densities to assess if apical densities or rhizome branch frequencies in 1998 correlated with changes in short-shoot density between 1998 and 1999.

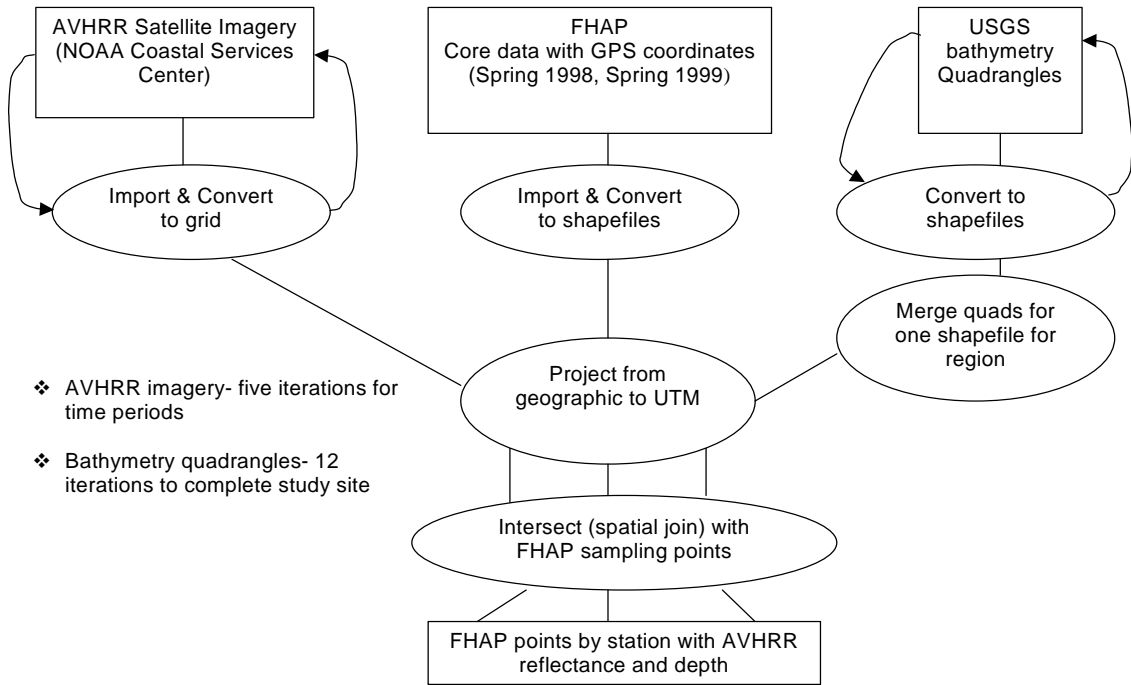
Bathymetry

The US Geological Survey performed bathymetric soundings in 1990 for the purpose of sedimentation and circulation dynamics for future modeling of Florida Bay (www.sofia.usgs.gov). Previous to this effort, bathymetry of Florida Bay had not been physically mapped in over a century. This study utilized the USGS bathymetry data since the depths taken from FHAP sampling at every station are based on PVC pole soundings and do not take sea level into account.

Arc/Info, a Geographic Information Systems (GIS) program was used to import and geographically organize the USGS bathymetric data (Fig. 2), which consisted of 7.5 minute X 7.5 minute quadrangles (ESRI 2000). These quadrangles can be visualized as spatial 'puzzle pieces' containing latitude (x), longitude (y), and the depth measurements (z) in meters. This study incorporated 12 quadrangles that covered the study area within the Everglades National Park boundaries.

Figure 2

Flow chart illustrating importation and manipulation of AVHRR, morphometrics, and bathymetric data into GIS, for exportation into spreadsheets



Determination of Light Availability

Attenuation coefficients have been shown to fluctuate among shallow, estuarine water bodies relative to wind speed and protection (Onuf 1996). Because of the variability associated with point sample methods (e.g. time of day, wind, cloud cover, etc.), a synoptic estimation of water clarity in relation to seagrass abundance was developed (Stumpf et al. 1999). These authors examined water clarity in Florida Bay from 1985 to 1997 and found changes in seagrass cover were inversely correlated with reflectance (a proxy for attenuation) measured using remotely sensed Advanced Very High Resolution Radiometer (AVHRR) spectral reflectance data. The more turbid the water, the higher the reflectance and the less light available for photosynthesis.

Three methods were used in this study to estimate optical water clarity at each station: secchi depth, light profiles of irradiance measured using scalar quantum sensors, and diffuse attenuation coefficients calculated from AVHRR data.

The relationship between Secchi depth and light attenuation is expressed as:

$$Z_s = u / K_d$$

where K_d = is the diffuse attenuation coefficient in m^{-1}
 Z_s = secchi depth in m
 u , a constant, 1.7 (Tilzer 1988)

Diffuse attenuation coefficients can more accurately be estimated from light profiles obtained *in situ* using scalar (4-pi) quantum sensors to measure photosynthetic photon flux densities (PPFD, photons $m^{-2} sec^{-1}$). Because of the characteristically shallow depths of Florida Bay (mean depth <2 m), K_d was

determined in 1999 using a sensor frame that maintained a fixed vertical separation (0.5 m) of 2 scalar sensors. Measurements of PPFD were obtained with the frame at two depths: (1) with the top sensor just below the surface and (2) with the bottom sensor just above the seagrass canopy. Diffuse attenuation coefficients were calculated using the Beer-Lambert Law:

$$K_d = \ln(I_o/I_z)/(\text{depth } o - \text{depth } z)$$

Where I_o = PPFD at top sensor
 I_z = PPFD at bottom sensor at depth $o + z$
 z = vertical separation of the 2 sensors

AVHRR imagery are considered raster data, containing digital numbers (DN) located within pixels of the imagery. Arc/View geoprocessing extensions allowed for reflectance values to be spatially joined into an attribute table, thus assigning a reflectance number to every FHAP station in the study area (Fig. 2).

Reflectance values were calculated by:

$$R_o = ((DN-1)/20)$$

Reflectance values (R_o) from the imagery were converted into attenuation values (K_d) using the algorithms of Stumpf et al. (1999). Since the relationships between R_o and K_d varied based on pigment concentration, the Bay was divided into two chlorophyll regimes (Stumpf et al. 1999). The Northwestern Bay region was characterized by high chlorophyll (concentrations over 5 ug/L). The eastern Bay region exhibited low chlorophyll concentrations (under 1 ug/L). Attenuation coefficients (K_d) were calculated from the reflectance data for low and high chlorophyll basins.

Low Chlorophyll	$R_o = 9.6 * K_d + 1.2$
High Chlorophyll	$R_o = 3.2 * K_d + 1.4$

Percent surface irradiance at the bottom of the Bay was used as the index of light availability and was calculated with the Beer-Lambert Law, using K_d from the AVHRR data and the recent USGS bathymetry data (Fig. 2).

$$S I = e^{-K_d(Z)}$$

Where Z = USGS depth in m

K_d = attenuation coefficient in m^{-1}

Previous shading studies of *Thalassia* suggest responses to reduced light are delayed, due to this species' extensive stored reserves (Hall et al. 1991). Thus, the AVHRR imagery and geoprocessing calculations were compiled and repeated for the several time periods antecedent to the spring 1998 sampling: the winter of 1997 (consisting of December, January, February, and March 1997), a yearly average of 1997 (consisting of all twelve months), a 3-month average of 1998 (consisting of February, March and April), the month of April 1998, considered to be one of two 'transition' months before 'summertime' begins, and the month of May 1998, when the FHAP sampling was done. These time periods were examined to determine what time period was most relevant to the relationship between light availability, short-shoot density, apical density or rhizome branch frequency.

Statistics

Since this study focused on the density of *T. testudinum*, only cores that contained *Thalassia* were used in analyses. T-tests were used to compare between-year variation in shoot and apical densities, rhizome branch frequency, secchi depths, and to compare variation in light attenuation coefficients (K_d)

obtained from light sensors in 1999 versus those calculated through AVHRR imagery for 1998. The Mann-Whitney Rank Sum test was used when data did not satisfy parametric assumptions. Mean short-shoot density, apical density, and rhizome branch frequency did not vary between sampling years. Thus, both sampling years were pooled for regression analyses across the study site.

Regression analyses related apical densities to short-shoot densities, and rhizome branch frequencies to short-shoot densities across the study site. Regressions were also used to compare relationships between rhizome branch frequency in 1998 and change in short-shoot densities from the spring of 1998 and 1999.

Multiple linear regressions tested which structural characteristic (short-shoot density, apical density, or rhizome branch frequency) would be the better response variable as a function of depth and light availability of the five time periods estimated from the AVHRR imagery across the study site. Linear regressions compared the variable with the best fit to the five AVHRR time periods to detect which time period was most relevant. Data were either arcsine (square root) or square root transformed to satisfy parametric assumptions during regressions. All statistics were performed using Sigma Stat 3.0 with significance determined at the 95% probability level (San Rafael, CA).

RESULTS

Mean short-shoot and apical densities and rhizome branch frequencies were not significantly different between the spring '98 and '99 samples (Table 1).

Light attenuation estimated from the secchi depths were also similar, suggesting similar optical water quality between the two years. However, at most stations the secchi disk was visible on the bottom. The secchi depth was less than the water depth at only 60 and 56 sites out of 314, 318 stations during 1998 and 1999 sampling, respectively (Table 1). This indicated relatively high light availability across most of the Bay during the two sampling periods. A comparison between K_d from AVHRR imagery for May 1998 and K_d values obtained from the spring 1999 light profiles also indicated similar optical water quality between years, at the bay scale (Table 1). However, even after removing several outliers, comparing station-level K_d values between the two datasets for 1998 (AVHRR) and 1999 (Light Profiles) indicated a high degree of station-to-station variability between the two datasets, suggesting a high degree of sub-pixel variability (Fig. 3). Remotely sensed estimates did not closely agree with in situ data at the station scale.

Comparisons between the square-root of apical densities and the square-root of short-shoot densities of pooled '98 and '99 core sample data (Table 2) indicated a positive relationship (Fig. 4), explaining 41% of the model variability across the study site (Eq. 1). The relationship between rhizome branch frequency and short-shoot densities across all basins was also positive (Eq. 2), but with a very weak fit ($R^2 = 0.02$). This is due to the large number of cores with one-to-several short-shoots, but without apical meristems (Fig. 5a). The core data where both short-shoots and apicals were present were examined (Fig. 5b) to determine if any possible relationship between rhizome branch frequency and

Table 1
 Mean (\pm SE) of different variables from t-tests of the spring of 1998 and the spring of 1999

Variable	Spring 1998 (Mean \pm SE)	Spring 1999 (Mean \pm SE)	df	t
<i>Morphometrics</i>				
Shoot Density (short-shoots*m ⁻²)	453.3 \pm 26.2	441.5 \pm 25.4	441	0.322
Apical Density (apicals*m ⁻²)	80.5 \pm 6.8	69.4 \pm 5.5	441	1.788
Branch Frequency (apicals/short-shoots)	0.19 \pm .02	0.15 \pm .01	441	2.044 ^a
<i>Water Depth</i>				
USGS (cm)	188.82 \pm 10.80	NS		NA
Secchi Depth (m ⁻¹) ^b	1.55 \pm .095	1.48 \pm .069	112	0.4143
Light Profile (m ⁻¹)	NS	0.58 \pm .030		NA
AVHRR (m ⁻¹)	.54 \pm .021	NS		NA

a t-test did not pass normality or constant variance. Mann-Whitney Rank Sum test indicated T = 47958, Median 0.11, 0.11 (1998, 1999 resp), p = 0.407.

b 60 out of 314, 56 out of 318 stations were of use (1998, 1999 resp) due to secchi disk being visible on bottom at most stations.

NS – not sampled, NA – not available, *p < .05.

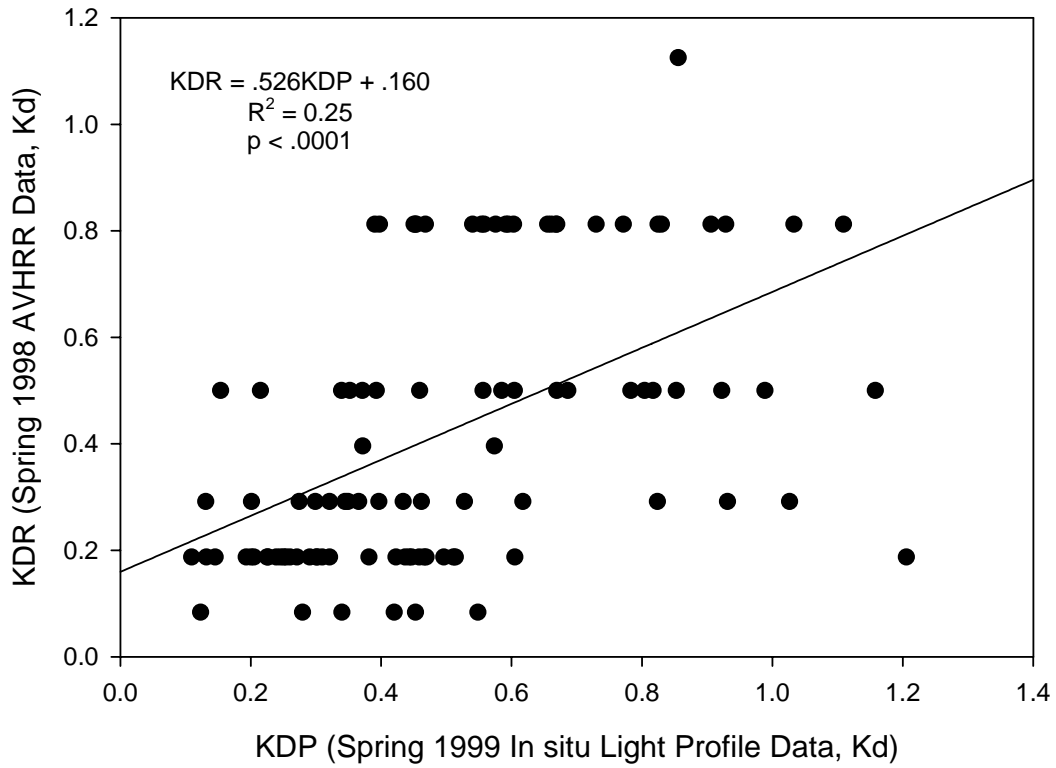


Figure 3
 Linear regression of light attenuation, K_d , obtained from May 1999 light profile data using quantum sensors (KDP) and AVHRR data from May 1998 (KDR)

Table 2
 Summary of linear regression analyses for the morphometric relationships between short-shoot density (SSD), apical density (APD), and rhizome branch frequency (BF) or apical density

Dependent Variable		Equation	Regression Statistics ^a		
Eq#			F	RSD	R ²
<i>Pooled Density</i>					
1	APD ^s	APD = 0.456SSD ^s - 2.62	305.61***	20.90	0.41
2	BF ^t	BF = 0.32SSD ^s + 12.4	8.06**	392.43	0.02
3	BF ^t	BF = -1.12SSD ^s + 57.9	125.26***	171.43	0.33
<i>Low Density</i>					
4	APD ^s	APD = 0.20SSD ^s + 5.86	11.46**	3.53	0.13
5	BF ^t	BF = -4.38SSD ^s + 106.7	93.03***	208.39	0.54
<i>High Density</i>					
6	APD ^s	APD = 0.27SSD ^s + 4.49	51.44***	9.96	0.23
7	BF ^t	BF = -0.006SSD ^s + 30.73	12.05**	65.64	0.06
<i>Density Changes</i>					
8	DEL SSD	DEL = - 0.004APD + 0.813	11.02**	2.41	0.06
9	DEL SSD	DEL = 1.09BF + 0.275	4.94*	2.49	0.03

DEL = changes in short-shoot density from the spring of 1998 to the spring of 1999, APD = apical density, SSD = short-shoot density, BF = rhizome branch frequency.

Low density consisted of all short-shoot densities between 0 – 350 short-shoots/m².

High density consisted of all short-shoot densities over 350 short-shoots/m².

a F-test, test of the mean square of the regression over the mean square of the residual error variance (RSD) (df = 440, 255, 80, 174 for pooled, extracted, low, and high densities, resp; 181 for density changes). Significant tests in bold, * p < .05, ** p ≤ .005, *** p ≤ .0001.

s square-root transformed.

t arcsine square root transformed..

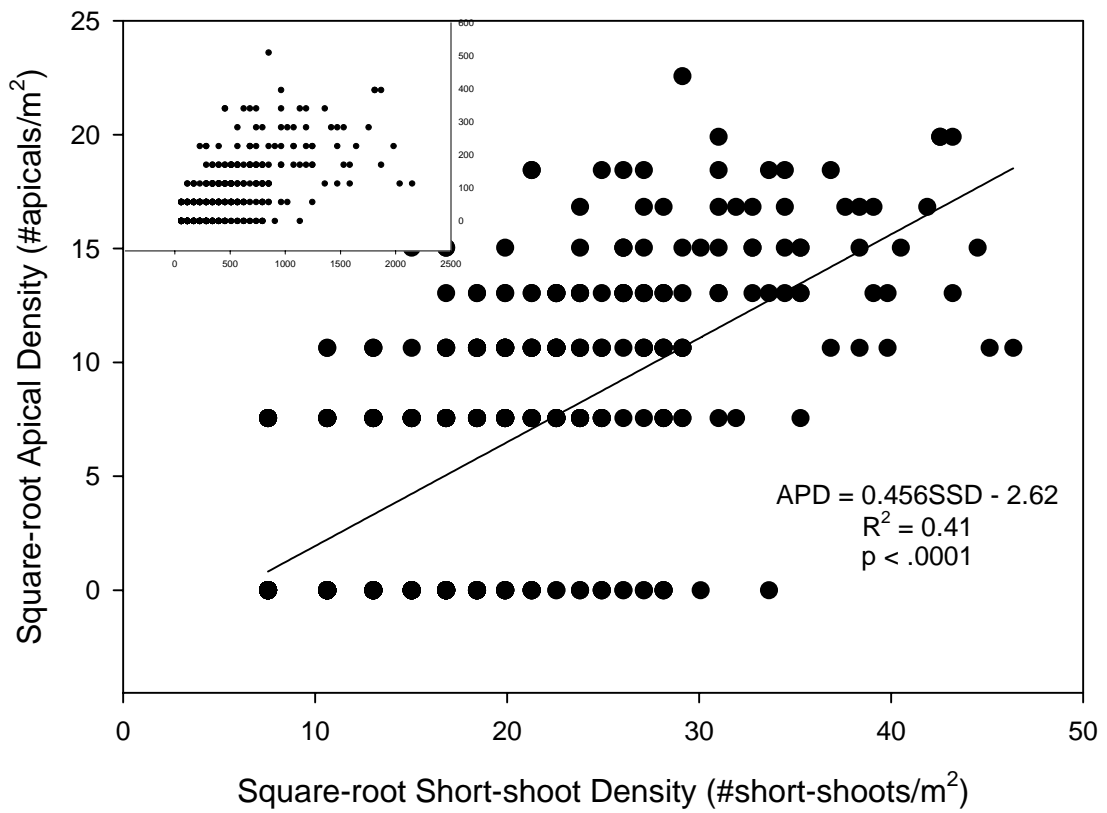


Figure 4
 Linear regression of the square root of apical densities (APD) and the square root of short-shoot densities (SSD) (raw data inset)

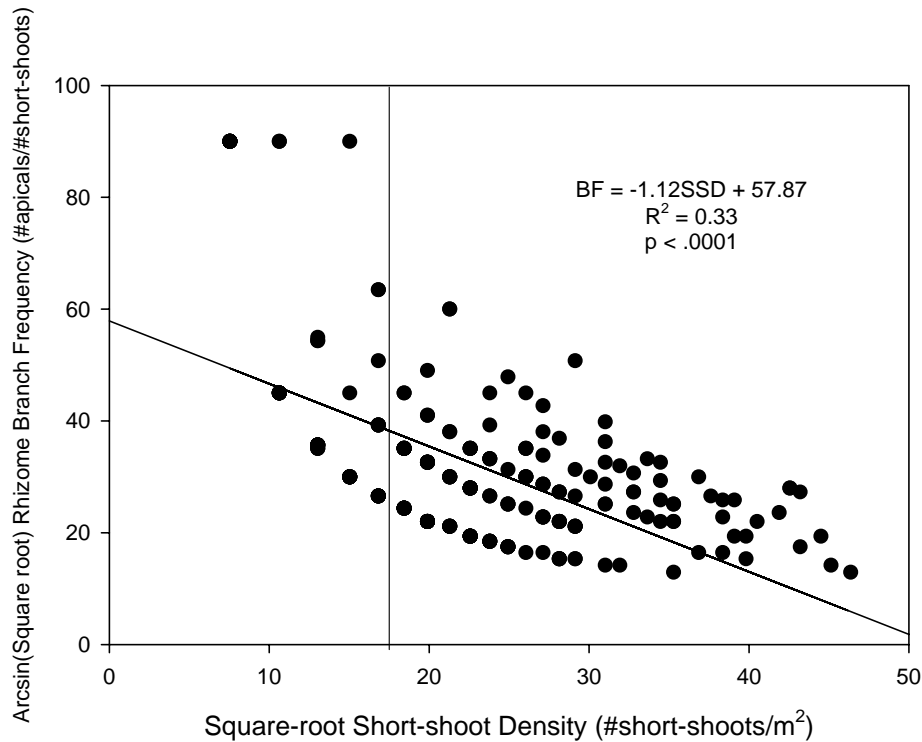
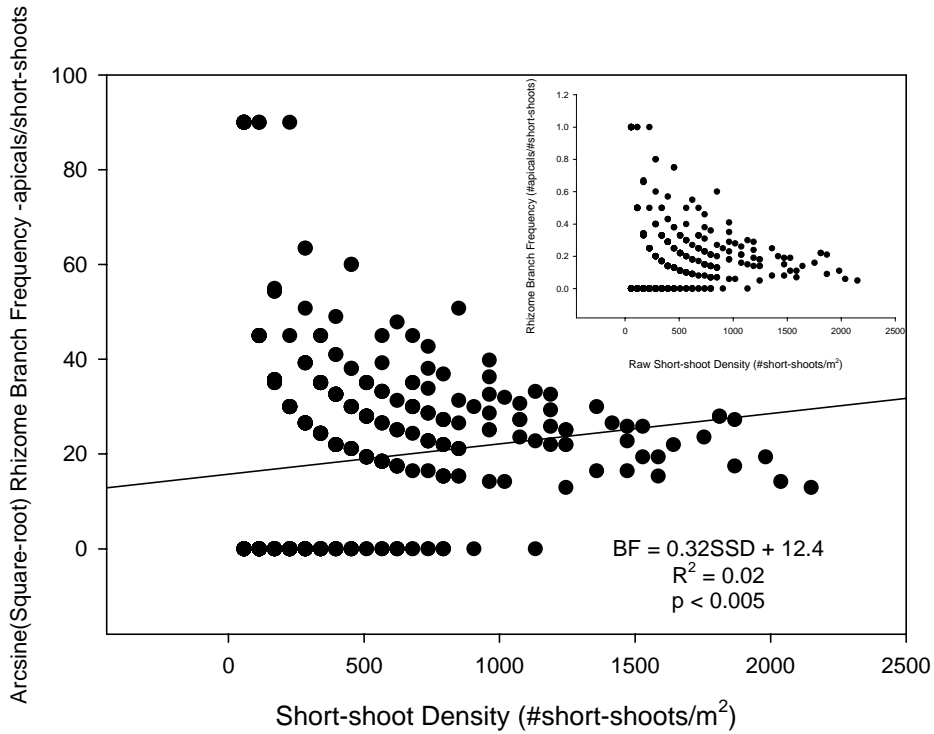


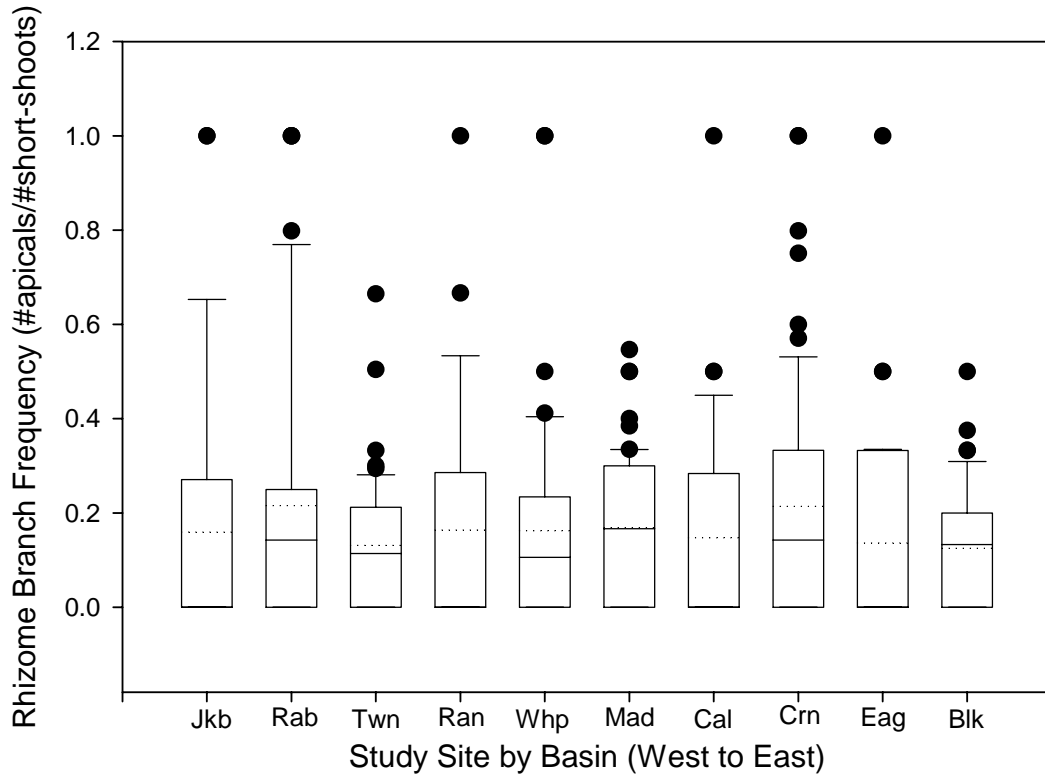
Figure 5
 Linear regression of (a) arcsine square root transformed rhizome branch frequency (BF) and short-shoot density (SSD) –327 data pts hidden (raw data inset) and (b) linear regression of BF and square root transformed SSD where only apical density and short-shoot density occur together – 155 data pts hidden

short-shoot density existed. A linear regression indicated a stronger negative relationship ($R^2 = 0.33$), explaining 33% of the model variation (Eq. 3).

A second series of regressions were performed to examine if there was a step-wise, density-dependent relationship between short-shoot densities versus apical densities and rhizome branch frequencies for low versus high short-shoot densities (Fig. 5b). Linear regression of square root apical densities and square root short-shoot densities for low shoot densities (0-350 ss/m²) indicated a lower R^2 value (0.13) than at higher shoot densities (0.23), but with similar slopes (Eq. 4, 6). Regressions of arcsine square root rhizome branch frequency and short-shoot density for low shoot densities explained approximately 54% of the model variation (Eq. 5), showing a strong negative association with rhizome branching at low short-shoot densities. The regression of arcsine square root rhizome branch frequency and square root short-shoot density at high short-shoot densities (> 350 ss/m²) indicated a near-zero negative slope and a very weak fit ($R^2 = 0.06$) (Eq. 7).

Further investigation into regressions of rhizome branch frequency and short-shoot densities were considered between basins. However, lack of *Thalassia* in several cores resulted in extreme differences in sample sizes. Although similar negative associations between rhizome branch frequency and short-shoot densities were observed in 8 out of 10 basins, comparisons would violate parametric assumptions, and inflate both Type I and II errors. Box plots of rhizome branch frequency by basin did not indicate any spatial trends (Fig. 6).

Figure 6
 Box plot illustrating the mean (dashed line), median (solid line), quartiles, and outliers (dots) of rhizome branch frequency by basin (geographic distance from west to east)



A regression of spring 1998 apical density and changes in short-shoot densities from 1998 to 1999 exhibited a very weak negative linear relationship (Table 2, Eq. 8). In contrast, comparing spring 1998 rhizome branch frequency and changes in short-shoot densities from 1998 to 1999 indicated a very weak positive linear relationship (Fig. 7, Table 2, Eq. 9).

Rhizome branch frequency did not vary significantly with water depth at the Bay scale (Table 3, Eq. 10). Multiple linear regressions performed between short-shoot density, apical density, and rhizome branch frequency versus light attenuation (K_d), calculated from five AVHRR time frames (KDR) indicated that square root short-shoot density was the best response variable to water clarity (Table 3, Eq. 11-15). Multiple linear regressions between short-shoot density, apical density, and rhizome branch frequency versus percent surface irradiance calculated for the five AVHRR time frames also indicated square root short-shoot density to be the best response variable to available light at depth (Eq. 21-25).

Linear regressions of optical water quality, K_d , calculated for the five AVHRR time frames revealed negative relationships with short-shoot densities (Eq. 16-20). Percent surface irradiance calculated for the five AVHRR time frames revealed positive relationships with short-shoot densities (Eq. 26-30). Both K_d and percent surface irradiance revealed the strongest fit ($R^2 = 0.26, 0.30$ resp) using the winter of 1997 data set (Eq. 19, 29 resp).

A small percentage of stations from each of the five time frames had potentially light-limiting conditions ($< 15\%$ SI). The three-month average of 1998

Table 3

Summary of multiple or linear regression analyses for the physical relationships between light attenuation (KDR), percent surface irradiance (SI), and short-shoot density (SSD), apical density (APD), or rhizome branch frequency (BF); and linear regression of water depth (USGS) and BF

	Physical Variable	Linear Regression Equation or MLR results (p value)	Regression Statistics ^a		
			F	RSD	R ²
10	<i>Water Depth</i> (USGS) <i>AVHRR</i> (KDR)	BF = 0.000002USGS + 0.285	0.001	0.046	0.00
	Multiple Regression				
11	May 1998	SSD(.001), APD(.51), BF(.66)	6.36**	0.075	0.07
12	April 1998	SSD(.001), APD(.93), BF(.86)	9.48**	0.087	0.12
13	Three Month	SSD(.001), APD(.50), BF(.68)	14.98**	0.145	0.15
14	Winter 1997	SSD(.001), APD(.56), BF(.21)	23.24**	0.152	0.20
15	Year 1997	SSD(.001), APD(.39), BF(.06)	18.57**	0.087	0.18
	Best Response				
16	May 1998	SSD ^s = -12.96SI + 17.3	27.84**	118.6	0.10
17	April 1998	SSD ^s = -14.29SI + 18.1	43.21**	98.09	0.16
18	Three Month	SSD ^s = -12.86SI + 22.6	67.63**	108.9	0.20
19	Winter 1997	SSD ^s = -13.72SI + 22.3	99.11**	99.44	0.26
20	Year 1997	SSD ^s = -17.22SI + 21.6	83.59**	98.09	0.24
	% <i>Surface Irradiance</i>				
	Multiple Regression				
21	May 1998	SSD(.001), APD(.73), BF(.61)	6.56**	369.2	0.07
22	April 1998	SSD(.002), APD(.41), BF(.78)	12.36**	362.7	0.15
23	Three Month	SSD(.001), APD(.32), BF(.47)	16.47**	283.1	0.16
24	Winter 1997	SSD(.001), APD(.84), BF(.25)	30.82**	342.9	0.25
25	Year 1997	SSD(.001), APD(.98), BF(.07)	18.93**	334.6	0.18
	Best Response				
26	May 1998	SSD ^s = 2.25SI - 4.07	22.71**	120.9	0.08
27	April 1998	SSD ^s = 2.92SI - 8.58	43.38**	108.6	0.17
28	Three Month	SSD ^s = 3.24SI - 4.48	64.58**	109.9	0.20
29	Winter 1997	SSD ^s = 3.60SI - 8.04	114.5**	95.5	0.30
30	Year 1997	SSD ^s = 2.98SI - 6.67	56.27**	108.6	0.18

USGS = bathymetry, KDR = light attenuation, Kd, SI = percent surface irradiance, BF = rhizome branch frequency, MLR = multiple linear regression (p-value in parentheses).

^a F-test, test of the mean square of the regression over the mean square of the residual error variance (RSD) (df = 254 for water depth, 247 for May 98, 221 for April 98, 266 for three-month average 98, 278 for Winter 97, and 264 for Year 97). Significant tests in bold, * p < .05, ** p ≤ .005, *** p ≤ .0001.

s square-root transformed.

showed 47 out of 266 stations to have less than 15% SI. The winter of 1997 average showed 39 out of 278 stations with less than 15% SI. The three other time frames had less than 2% of their stations that exhibited light-limiting conditions. Regressions were used to analyze the relationship between short-shoot density or rhizome branch frequency and available light for the three month average (Feb. Mar. Apr. 1998) time frame since it had the largest percentage of stations containing less than 15% SI. Short-shoot densities were observed to increase with available light (Fig. 8a). In contrast, rhizome branch frequency decreased with increasing available light (Fig 8b).

DISCUSSION

Optical water quality is generally thought to be a limiting factor for seagrass density. Shallow, coastal seagrass meadows have a maximum depth congruent to the secchi depth (Gallegos and Kenworthy 1996; Carruthers and Walker 1999) although the maximum depth of seagrass may be 1.7 - 2 times the measured secchi depth. Results from this study suggest that seagrass growth in Florida Bay was not generally light limited during spring 1998 and spring 1999, as secchi depths were greater than water depths in most of the Bay (Table 1). This may explain the lack of a relationship between rhizome branch frequency and water depth (USGS bathymetry) across the study site.

Previous research has suggested a coupling between turtle grass shoot production and apical densities (Marba and Duarte 1998, Duarte and Sand-Jensen 1990; Durako 1995). Apical and short-shoot densities were linearly

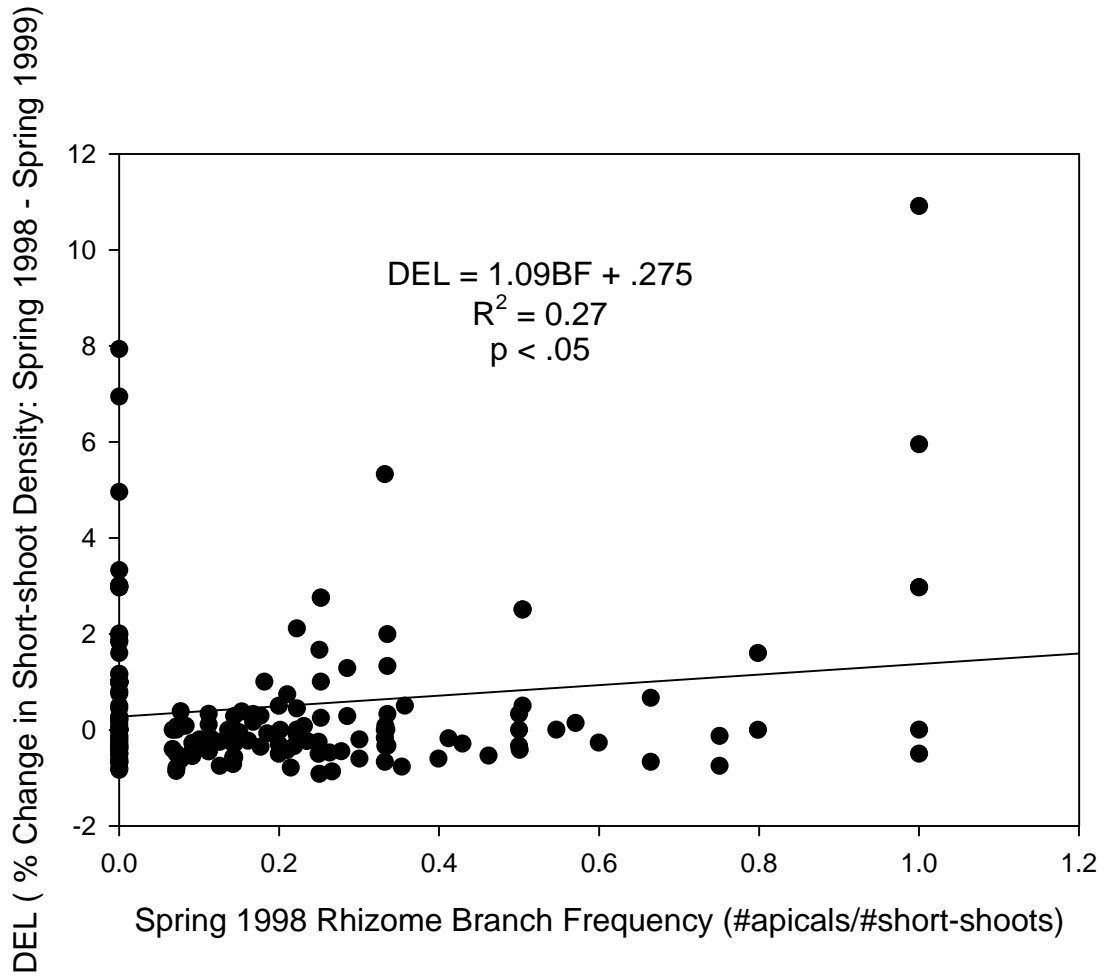


Figure 7
 Linear regression of rhizome branch frequency (BF) and the differences in short-shoot densities (DEL) from the spring of 1998 and the spring of 1999

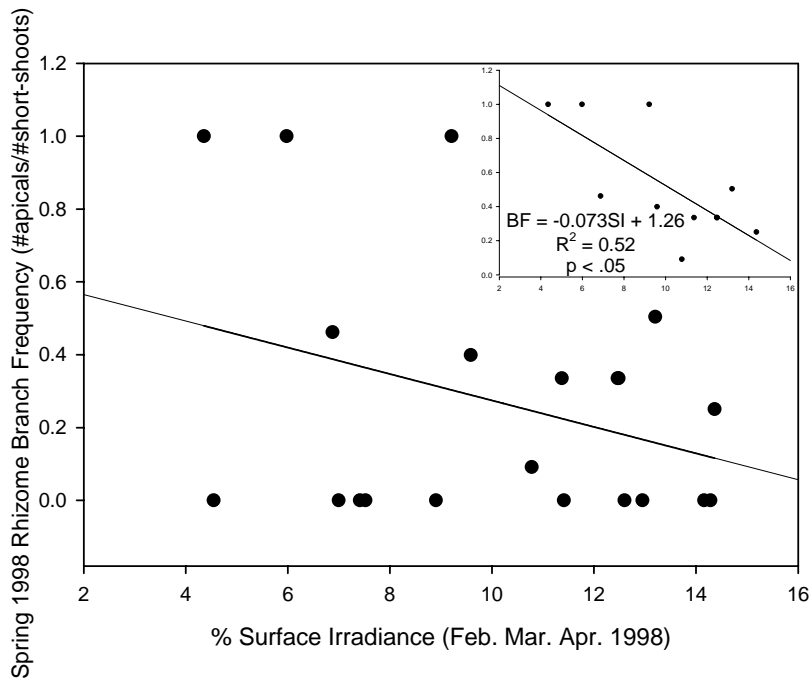
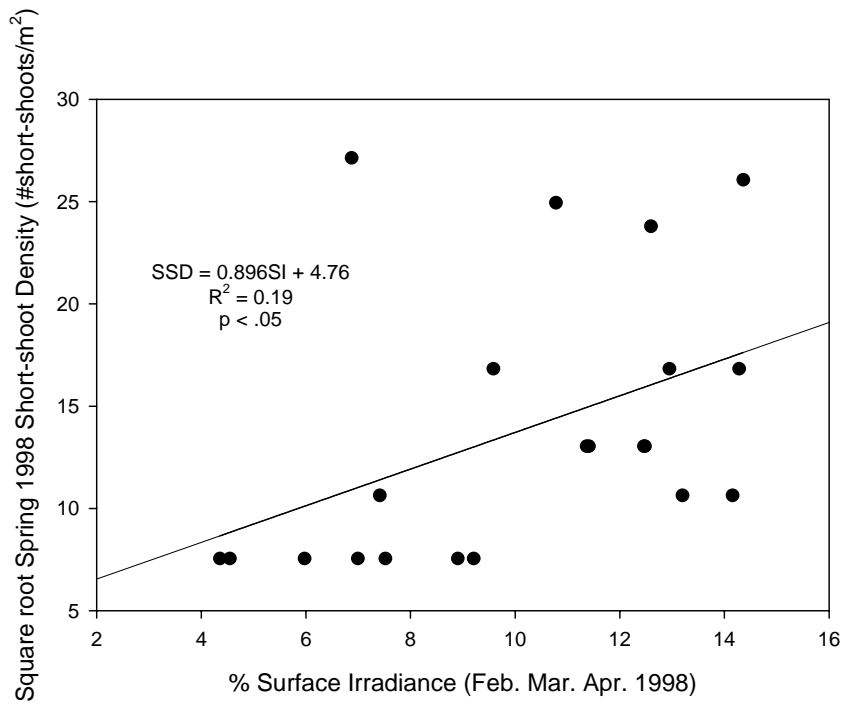


Figure 8
 Linear regression of (a) spring 1998 short-shoot density (SSD) and %SI (three month average 1998) for stations where % SI < 15 and (b) linear regression of spring 1998 rhizome branch frequency (BF) and % SI for stations where SI < 15% (three month average 1998) (inset excludes 10 cores with short-shoots only)

correlated in Florida Bay (Fig. 4). However, rhizome branch frequency, defined as a ratio of apical meristems to short-shoots, displayed several responses when compared to short-shoot density (Fig. 5a,b). There were two situations that changed the slope and model variation. The core data analyzed during this study either had apical meristems and short-shoots present or they had only short-shoots. Analyzing the subset of cores that had both short-shoots and apical meristems was done to determine if there was a relationship when branching was present. In this case, rhizome branch frequency exhibited a negative relationship with short-shoot density, exhibiting a rapid decline in rhizome branching up to moderate short-shoot densities (350 short-shoots/m², Fig. 5b). Thus, rhizome branch frequency may have a stronger negative relationship with short-shoot density at lower densities than at high short-shoot densities (Table 3, Eq. 5, 7). The three 'curved' lines observed in Fig. 5a,b are an artifact of the ratio used to calculate rhizome branch frequency combined with the multiplier used for density conversion from cm² to m². In contrast to branch frequency, apical densities exhibited a stronger positive relationship with increasing shoot densities (Table 2, Eq. 4, 6). These results are consistent with Durako (1995), who suggested apical density was dependent on short-shoot density.

Neither apical density nor rhizome branch frequency in 1998 was found to be a good predictor of short-shoot density fluctuations between the spring of 1998 and 1999 (Table 2, Eq. 8,9). Increases in rhizome branch frequencies were only weakly associated with between-year increases in short-shoot densities in this study (Fig 7). Mean rhizome branch frequencies were 0.19 ± 0.02 , and 0.15

± 0.01 , for spring 1998 and spring 1999, respectively (Table 1). Previous observations of *T. testudinum* in Florida Bay reported similar rhizome branch frequencies near 0.25 in areas affected by die-off (Durako 1995). Rollon et al. (2001) found similar apical meristem production among young *Thalassia hemprichii* populations. Calculated rhizome branch frequencies were 0.12 and 0.18 for two different sites considered to be rapidly expanding. A study in Tampa Bay, Florida found apical meristems to be significantly more abundant in areas disturbed from propeller scars, with a large percentage of rhizome apices near scar edges, and angled toward the disturbance (Dawes et al. 1997). The relatively lower rhizome branching rates observed in Florida Bay in 1998 and 1999 may reflect a density-dependent inhibitory response due to the increase in short-shoot densities following the seagrass die-off from 1990 to 1998 (305 short shoots/m² in 1990, Durako 1995 versus 590 & 602 short shoots/m² in this study).

Light availability may also control carbon allocation to rhizome growth, apical production and rhizome branching. An in situ light reduction study that completely severed rhizome connections between shaded *Thalassia* plots and surrounding unshaded plots showed that rhizome biomass decreased to 50% of the original biomass, after 490 days (Lee and Dunton 1997). However, Hall et al. (1991) found leaf growth in *Thalassia* in shaded plots where shaded shoots remained connected to surrounding shoots was similar to their control plots after 13 months. These two studies show the importance of underground reserves and clonal integration in the lag in response in *Thalassia* between light reduction and growth reduction. *Thalassia testudinum* exploits several alternative growth

strategies in response to light reduction which may be affected by rhizome reserves and shoot density (Marba and Duarte 1998; Dawes et al. 1997). In this regard, rhizome branch frequency in Florida Bay during this study may have been density dependent.

A lag time between light reduction and short-shoot densities may be dependent on seagrass rhizome reserves. Seagrass studies involving light attenuation have observed K_d to be highly variable over time (Dennison 1987, Lee and Dunton 1997). This study only sampled in situ light attenuation from quantum sensors and secchi profiles twice a year, making it difficult to assess any temporal relationships. However the use of AVHRR reflectance imagery allowed for time-integrated, sequential and synoptic views of light attenuation among the FHAP stations. Weak negative relationships between rhizome branch frequency sampled in May '98 and percent surface irradiance were calculated using detailed bathymetry and satellite-based K_d . This suggests that rhizome branching decreases with increased light availability. The strongest relationship was between short-shoot density in 1998 and light availability for the Winter of 1997 time frame, indicating a few months lag time in this response in Florida Bay. There was a positive relationship between percent surface irradiance and short-shoot density (Fig. 8a). In conclusion, rhizome branch frequency was not a good ecoindicator of light availability or short-shoot density changes in Florida Bay. In contrast, it appears that the effect of short-shoot density, which did respond positively to increasing light availability, may be more important in effecting rhizome branching. Therefore, rhizome branch frequency may be a biological

indicator that responds to short-shoot density changes in this non-light limited Bay.

Literature Cited

- Brouns JJWM (1985) The plastochrone interval method for the study of the productivity of seagrasses; possibilities and limitations. *Aquat Bot* 21: 71-78
- Carruthers TJB, Walker DI (1999) Sensitivity of transects across a depth gradient for measuring changes in aerial coverage and abundance of *Ruppia megacarpa* Mason. *Aquatic Botany* 65: 281–292
- Dawes CJ, Andorfer JA, Rose C, Uranowski C, Ehringer N (1997) Regrowth of the seagrass *Thalassia testudinum* into propeller scars. *Aquat Bot* 59: 139-155
- den Hartog C (1970) Seagrasses of the World. *Verh K Ned Aka Wet Natuurk* 59(1): 275
- den Hartog C (1987) Wasting disease and other dynamic phenomena in *Zostera* beds. *Aquat Bot* 27: 3-14
- Dennison WC (1987) Effects of light on seagrass photosynthesis, growth and depth distribution *Aquat Bot* 27: 15-26
- Duarte CM, (1991) Seagrass depth limits. *Aquat Bot* 40: 363-377
- Duarte CM, Sand-Jensen K (1990) Seagrass colonization: Biomass development and shoot demography in *Cymodocea nodosa* patches. *Mar. Ecol Prog Ser* 67: 97-103
- Durako MJ (1994) Seagrass die-off in Florida Bay (USA): Changes in shoot demographic characteristics and population dynamics in *Thalassia testudinum*. *Mar Ecol Prog Ser* 110:59-66
- Durako MJ (1995) Indicators of seagrass ecological condition: An assessment based on spatial and temporal changes. In: Dyer KR, Orth RJ (ed) *Changes in fluxes in estuaries: Implications for science to management*. Olsen and Olsen, Fredensborg 261-266
- Durako MJ, Kuss KM (1994) Effects of *Labyrinthula* infection on the photosynthetic capacity of *Thalassia testudinum*. *Bull Mar Sci* 54(3): 727-732
- ESRI (2000) Earth Systems Research Institute Inc. Redlands, CA
- Fourqurean JW, Zieman JC (1991) Photosynthesis, respiration and whole plant carbon budget of the seagrass *Thalassia testudinum*. *Mar Ecol Prog Ser* 69: 161-170

- Gallegos CL, Kenworthy WJ (1996) Seagrass depth limits in the Indian River Lagoon (Florida, U.S.A.): Application of an optical water quality model. *Est Coast Shelf Sci* 42: 267–288
- Gallegos ME, Merino M, Marba N, Duarte CM (1993) Biomass and Dynamics of *Thalassia testudinum* in the Mexican Caribbean: Elucidating Rhizome Growth. *Mar Ecol Prog Ser* 95: 185-192
- Hall MO, Tomasko DA, Courtney FX (1991) Light Requirements of Seagrasses: Results and recommendations of a workshop held in West Palm Beach, Florida on November 7-8, 1990. NOAA Tech Memo #8970 187 pp
- Hall MO, Durako MJ, Fourqurean JW, Zieman JC (1999) Decadal changes in seagrass distribution and abundance in Florida Bay. In: Porter JW, Porter KG. *Estuaries* 22 (2B): 445-459
- Lee KS, Dunton KH (1997) Effects of in situ light reduction on the maintenance, growth and partitioning of carbon resources in *Thalassia testudinum* Banks ex Koenig. *J Exp Mar Biol Ecol* 210 (1): 53-73
- Linton DM, Warner GF (2003) Biological indicators in the Caribbean coastal zone and their role in integrated coastal management. *Ocean & Coastal Management* 46: 261–276
- Marba N, Duarte CM (1998) Rhizome elongation and seagrass clonal growth. *Mar Ecol Prog Ser* 174: 269-280
- Nichols PD, Klumpp DW, Johns RB (1982) Lipid components of the seagrasses *Posidonia australis* and *Heterozostera tasmanica* as indicators of carbon source. *Phytochemistry* 21(7): 1613-1621
- Onuf CP (1996) Seagrass responses to long-term light reduction by brown tide in Upper Laguna Madre, Texas: Distribution and biomass patterns. *Mar. Ecol Prog Ser* 138 (1-3): 219-231
- Orfanidis S, Panayotidis P, Stamatis N (2003) An insight to the ecological evaluation index (EEI). *Ecological Indicators* 3(1) 27-33
- Orth RJ, van Montfrans J (1990) Utilization of marsh and seagrass habitats by early stages of *Callinectes sapidus*: A Latitudinal Perspective. *Bull Mar Sci* 46(1): 126-144
- Phillips RC, Menez EG (1988) Seagrasses. *Smithsonian Contributions to the Marine Sciences #34*. Smithsonian Institution Press. Washington, DC

- Phlips EJ, Lynch TC, Badylak S (1995) Chlorophyll a, tripton, color, and light availability in a shallow tropical inner-shelf lagoon, Florida Bay, USA. *Mar Ecol Prog Ser* 127: 223-234
- Powell GVN, Kenworthy WJ, Fourqurean JW (1989) Experimental evidence for nutrient limitation of seagrass growth in a tropical estuary with restricted circulation. *Bull Mar Sci* 44: 324-340
- Robblee MB, Barber TR, Carlson Jr. PR, Durako MJ, Fourqurean JW, Muehlstein LK, Porter D, Yarbrow LA, Zieman RT, Zieman JC (1991) Mass mortality of the tropical seagrass *Thalassia testudinum* in Florida bay. *Mar Ecol Prog Ser* 71: 297-299
- Rollon RN, Cayabyab NM, Fortes MD (2001) Vegetative dynamics and sexual reproduction of monospecific *Thalassia hemprichii* meadows in the Kalayaan Island group. *Aquat Bot* 71: 239-246
- Short FT, Jones GE, Burdick DM (1991) Seagrass decline: Problems and solutions. Coastal Wetlands Coastal Zone Conference
- Stumpf RP, ML Frayer, Durako MJ, Brock JC (1999). Variations in Water Clarity and Bottom Albedo in Florida Bay from (1985) to (1997). *Estuaries* 22(2B): 431
- Terrados J, Duarte CM, Kenworthy WJ (1997) Experimental evidence for apical dominance in the seagrass *Cymodocea nodosa*. *Mar. Ecol Prog Ser* 148: 263-268
- Thayer GW, Wolfe DA, Williams RB (1975) The impact of man on seagrass systems. *American Scientist* 63(2): 288-296
- Tilzer MM (1988) Secchi disk-chlorophyll relationships in a lake with highly variable phytoplankton biomass. *Hydrobiologia* 162: 163-171
- Tomasko DA, Dawes CJ (1988) Depth distribution of *Thalassia testudinum* in two meadows on the west coast of Florida: A difference in the effect of light availability-PSZNI. *Marine Ecology* 9: 123-130
- Tomasko DA, Dawes CJ (1989) Evidence for the physiological integration between shaded and unshaded short shoots of *Thalassia testudinum*. *Mar. Ecol Prog Ser* 54: 299-305
- Tomasko DA, Dawes CJ (1990) Influences of season and water depth on the clonal biology of the seagrass *Thalassia testudinum*. *Mar Biol* 105(2): 345-351

- Tomasko DA, Dawes CJ, Hall MO (1991) The effects of the number of short shoots and presence of the rhizome apical meristem on the survival and growth of transplanted seagrass *Thalassia testudinum*. Cont Mar Sci 32: 41-48
- Tomasko DA, Dawes CJ, Hall MO (1996) The effects of anthropogenic nutrient enrichment of turtle grass (*Thalassia testudinum*) in Sarasota bay, Florida. Estuaries 19(2B): 448-456
- Tomasko DA, Lapointe BE (1991) Productivity and biomass of *Thalassia testudinum* as related to water column nutrient availability and epiphyte levels: Field observations and experimental studies. Mar. Ecol. Pro. Ser 75: 9-17
- Tomlinson PB (1974) Vegetative morphology and meristem dependence- The foundation of productivity in seagrasses. Aquaculture 4: 107-130
- Van Tussenbroek BI (1996) Integrated growth patterns of turtle grass, *Thalassia testudinum* Banks ex Koenig. Aquat Bot 55 (2): 139-144
- Van Tussenbroek BI, Galindo CA, Marquez J (2000) Dormancy and foliar density regulation in *Thalassia testudinum*. Aquat Bot 68: 281-295
- Zieman JC, Fourqurean JW, Iverson RI (1989) Distribution, abundance, and productivity of seagrass and macroalgae in Florida bay. Bull Mar Sci 44(1): 292-311

APPENDIX

Metadata

Advanced Very High Resolution Radiometer

Identification_Information:

Citation:

Citation_Information:

Originator:

National Ocean and Atmosphere Administration/ Coastal Services Center/ Coastal Ocean Remote Sensing group

Publication_Date: 19980809

Title:

Remotely sensed south Florida images of percent water reflectance and sea surface temperature derived from the Advanced Very High Resolution Radiometer (AVHRR)

Geospatial_Data_Presentation_Form: remote-sensing image

Publication_Information:

Publication_Place: Charleston, South Carolina, USA

Publisher: NOAA/CSC

Online_Linkage: <http://www.csc.noaa.gov>

Description:

Abstract:

Satellite imagery from NOAA polar orbiter environmental satellites has been converted to several products. Sea surface temperature (SST) has been calculated using a multichannel split window algorithm or a non-linear split window algorithm on the thermal channels (MCSST and NLSST algorithms). The percent reflectance in the red (a proxy for turbidity and suspended sediments) has been calculated using channels 1 and 2, with corrections for atmospheric aerosols and Rayleigh radiance and with calibrations based on the Pathfinder program to remove variation among satellites. A complete description of the AVHRR water reflectance derivation can be found in Stumpf and Pennock (1989) and Stumpf and Frayer (1997; see bibliography).

For near real-time reflectance and sea surface temperature imagery, visit the USGS Florida Bay homepage (<http://coastaler.usgs.gov/flbay/>) and the NOAA Coastal Services Center, Coastal Remote Sensing homepage (<http://www.cscnoaagov/crs/>).

Purpose:

All products provide a synoptic view of south Florida waters. They may be used for a variety of purposes, including determination of the location of thermal fronts and strong currents (with SST), or locating sediment plumes (with percent reflectance).

Supplemental_Information:

These images were created with the USGS program AVHRRMAP7. A scene specific image offset was subtracted from each daily reflectance image to compensate for residual drift in satellite calibration and individual scene reflectance deviations. The offset for an image was determined by averaging reflectance values from up to 22 locations in the Florida Current/Gulf Stream waters (depending on cloud cover). Reflectance in these clear water regions should always be close to zero. The final offset was taken as the average offset minus 1 standard deviation. The monthly and seasonal reflectance images were derived by averaging pixel-by-pixel the original uncorrected imagery (no offsets) for the time period of interest. Offsets for the monthly and seasonal images were then determined using the same method as described above for the individual scenes.

Filenames have the format YYMMDD??.gif or YYMMDD??.tif where YY = year, MM = month, DD = day of month, ?? = two character product identification: rf = reflectance; st = SST '.gif' extension files are in image GIF format. '.tif' extension files are GeoTIFFs that preserve radiometric pixel values (see Entity_and_Attribute_Overview)

Monthly averages have the format yyrefmimgif or .tiff where YY = year, and MM = month over which the average was calculated. Winter averages have a format of winyyrefgif or .tif while the summer averages have a format of sumyyrefgif or .tiff. Winter averages were calculated using all images from December - March, while summer averages were calculated using images from June - September.

Time_Period_of_Content:

Time_Period_Information:

Range_of_Dates/Times:

Beginning_Date: 19850707

Ending_Date: 19980529

Currentness_Reference: source imagery date

Status:

Progress: complete

Maintenance_and_Update_Frequency: None planned

Spatial_Domain:

Bounding_Coordinates:

West_Bounding_Coordinate: 83.07385 W

East_Bounding_Coordinate: 79.81552 W

North_Bounding_Coordinate: 26.10398 N

South_Bounding_Coordinate: 24.32936 N

Keywords:

Theme:

Theme_Keyword_Thesaurus: none

Theme_Keyword: AVHRR

Theme_Keyword: SST

Theme_Keyword: water clarity

Theme_Keyword: turbidity

Theme_Keyword: water reflectance

Theme_Keyword: sea surface temperature

Theme_Keyword: bottom albedo

Theme_Keyword: seagrass

Theme_Keyword_Thesaurus: GCMD

Theme_Keyword: EARTH SCIENCE > BIOSPHERE > Aquatic Habitat >

Coastal Habitat

Theme_Keyword: EARTH SCIENCE > BIOSPHERE > Water Quality >

Turbidity

Theme_Keyword: EARTH SCIENCE > BIOSPHERE > Water Quality > Water

Temperature

Theme_Keyword: EARTH SCIENCE > OCEANS > Ocean Optics > Turbidity

Place:

Place_Keyword_Thesaurus: none

Place_Keyword:

United States

Coast Place_Keyword: Florida Bay

Access_Constraints: Not suitable for navigation

Use_Constraints:

Data is approximately 1.1 km resolution it is not useful for projects requiring higher resolution. It is also subject to clouds covering the area of interest. Where the cloud cover algorithms fail due to partially cloudy pixels, typically seen as a ring around flagged clouds, the sea surface may appear colder than it should be and reflectance may appear stronger.

Data_Quality_Information:

Attribute_Accuracy:

Attribute_Accuracy_Report:

Where no clouds are present, SST should be within 0.5 degrees Celsius. Accuracy of reflectance product is unknown; precision where no clouds are present is 0.003 (or 0.3 %). The data has been navigated to +/- one pixel

Logical_Consistency_Report: N/A

Completeness_Report: done

Positional_Accuracy:
Horizontal_Positional_Accuracy:
Horizontal_Positional_Accuracy_Report: Generally within 1 kM

Lineage:

Source_Information:
Source_Citation:
Citation_Information:
Originator:
National Oceanic and Atmospheric Administration / National
Environmental Satellite, Data, and Information Service / National
Climatic Data Center / Satellite Data Services Division (Katherine B
Kidwell eD)
Publication_Date: 199506
Title: NOAA Polar Orbiter Data Users Guide Edition: June 1995
Publication_Information:
Publication_Place: Washington, DC
Publisher: NOAA/NESDIS/NCDC/SDSD
Online_Linkage: URL:http://saars3.saAnoaAgov:5726/pod_documents/
Type_of_Source_Media: CD - ROM
Source_Time_Period_of_Content:
Time_Period_Information:
Single_Date/Time:
Calendar_Date: 199506
Source_Currentness_Reference: current
Source_Citation_Abbreviation: PODUG
Source_Contribution: Describes the satellite system
Process_Step:
Process_Description: Sea Surface Temperature calculation
Process_Date: 19980809

Spatial_Data_Organization_Information:

Indirect_Spatial_Reference: United States
Direct_Spatial_Reference_Method: Raster
Raster_Object_Information:
Raster_Object_Type: Pixel
Row_Count: 178
Column_Count: 295

Spatial_Reference_Information:

Horizontal_Coordinate_System_Definition:
Planar:
Grid_Coordinate_System:
Grid_Coordinate_System_Name: Universal Transverse Mercator
Universal_Transverse_Mercator:
UTM_Zone_Number: 17 Tranverse_Mercator

Transverse_Mercator:

Scale_Factor_at_Central_Meridian: 0.99960

Longitude_of_Central_Meridian: -81.00

Latitude_of_Projection_Origin: 0.00

False_Easting: 500000.00

False_Northing: 0.00

Planar_Coordinate_Information:

Planar_Coordinate_Encoding_Method: row and column

Coordinate_Representation:

Abscissa_Resolution: 1100

Ordinate_Resolution: 1100

Planar_Distance_Units: meters

Geodetic_Model:

Horizontal_Datum_Name: NAD83

Ellipsoid_Name: GRS80

Semi-major_Axis: 6378137 meters

Denominator_of_Flattening_Ratio: 298.257

Entity_and_Attribute_Information:

Overview_Description:

Entity_and_Attribute_Overview:

The calculated sea surface temperature and percent reflectance are derived from rescaled 8 bit AVHRR data. The integer 8 bit (DN) values rescale to temperature as $\text{Temp (degrees Celsius)} = (\text{DN} - 30)/6$. The percent reflectance is scaled as $\text{Reflectance (\%)} = (\text{DN} - 1)/20$.

Entity_and_Attribute_Detail_Citation: Originator defined

Distribution_Information:

Distributor:

Contact_Information:

Contact_Organization_Primary:

Contact_Organization: NOAA Coastal Services Center

Contact_Address:

Address_Type: mailing and physical address

Address: 2234 South Hobson Avenue

City: Charleston

State_or_Province: SC

Postal_Code: 29405-2413

Contact_Voice_Telephone: none

Resource_Description: AVHRR images processed to SST and reflectance

Distribution_Liability: None, use at own risk

Metadata_Reference_Information:

Metadata_Date: 19980809

Metadata_Contact:

Contact_Information:

Contact_Organization_Primary:

Contact_Organization: NOAA Coastal Services Center

Contact_Address:

Address_Type: mailing and physical address

Address: 2234 South Hobson Avenue

City: Charleston

State_or_Province: SC

Postal_Code: 29405-2413

Country: USA

Contact_Voice_Telephone: None

Metadata_Standard_Name: FGDC Content Standards for Digital Geospatial
Metadata

Metadata_Standard_Version: 19940608

High-Resolution Bathymetry of Florida Bay

- * Identification_Information
- * Data_Quality_Information
- * Distribution_Information
- * Metadata_Reference_Information

Identification_Information:

Citation:

Citation_Information:

Originator: Mark Hansen

Publication_Date: Unpublished material

Title: High-Resolution Bathymetry of Florida Bay

Publication_Information:

Publication_Place:

Publisher:

Online_Linkage:

Description:

Abstract:

The bathymetry of Florida Bay has not been systematically mapped in 100 years. New bathymetric data are being collected to help assess sedimentation rates and to provide a foundation for a sediment budget and circulation model for the Bay. As part of this effort new techniques are being used to collect highly accurate data in shallow water, and to provide bank-top and tidal flat elevation data that previously were unavailable.

Purpose:

Detailed, high-resolution maps of Florida Bay mudbank elevations are needed to understand sediment dynamics and provide input into circulation models. An accurate bathymetric survey will provide a baseline for assessing future sedimentation rates in Florida Bay (sediment movements associated with storms, seasonal accretion, erosion patterns) and a foundation for developing a sediment budget.

Supplemental_Information: none

Time_Period_of_Content:

Time_Period_Information:

Range_of_Dates/Times:

Beginning_Date: 1995

Ending_Date: 1999

Currentness_Reference: Publication date

Status:

Progress: in work

Maintenance_and_Update_Frequency: as needed

Spatial_Domain:

Bounding_Coordinates:

West_Bounding_Coordinate: -81.17

East_Bounding_Coordinate: -80.33

North_Bounding_Coordinate: 25.25
South_Bounding_Coordinate: 24.75

Keywords:

Theme:

Theme_Keyword_Thesaurus: none
Theme_Keyword: High-resolution maps
Theme_Keyword: Sediment dynamics
Theme_Keyword: Circulation models
Theme_Keyword: System for Accurate nearshore Depth Surveying
Theme_Keyword: SANDS
Theme_Keyword: Global positioning
Theme_Keyword: Drainage patterns

Place:

Place_Keyword_Thesaurus: none
Place_Keyword: Florida Bay
Place_Keyword: Everglades National Park
Place_Keyword: Buttonwood embankment
Place_Keyword: Florida Keys
Place_Keyword: Central Everglades

Access_Constraints: none

Use_Constraints: none

Point_of_Comments and suggestions? Contact:

Contact_Information:

Contact_Person_Primary:

Contact_Person: Mark Hansen

Contact_Organization: US Geological Survey

Contact_Position: Oceanographer

Contact_Address:

Address_Type: mailing address

Address: 600 Fourth Street South

City: St. Petersburg

State_or_Province: FL

Postal_Code: 33701

Contact_Voice_Telephone: 727 893 3100 ext 3036

Contact_Facsimile_Telephone: 727 893 3333

Contact_Electronic_Mail_Address: mhansen@usgs.gov

Hours_of_Service:

Browse_Graphic:

Browse_Graphic_File_Name:

Browse_Graphic_File_Description:

Browse_Graphic_File_Type:

Data_Set_Credit:

Native_Data_Set_Environment:

Data_Quality_Information:

Logical_Consistency_Report: not applicable

Completeness_Report: not applicable

Positional_Accuracy:

Horizontal_Positional_Accuracy:

Horizontal_Positional_Accuracy_Report: not available

Quantitative_Horizontal_Positional_Accuracy_Assessment:

Horizontal_Positional_Accuracy_Value: 0.05 cm

Horizontal_Positional_Accuracy_Explanation: not available

Vertical_Positional_Accuracy:

Vertical_Positional_Accuracy_Report: not available

Quantitative_Vertical_Positional_Accuracy_Assessment:

Vertical_Positional_Accuracy_Value: 0.10 cm

Vertical_Positional_Accuracy_Explanation: not available

Lineage:

Process_Step:

Process_Description:

Differential Global Positioning System (DGPS) techniques will be employed via shallow-draft boats to map the bathymetry of subtidal embayments between the mangrove fringe and the Buttonwood embankment to provide high-quality elevation data needed in support of simulation model development. Extension of methods to define tidal creek drainage patterns and relief gradients through the mangrove fringe will also be investigated.

The US Geological Survey (USGS) has developed a System for Accurate Nearshore Depth Surveying (SANDS) that is accurate to 10 cm vertically/6 cm horizontally and can survey in depth as little as 30 cm. The entire Bay has been divided into roughly 18 USGS 1:24,000 quadrangles and will be mapped over a five-year period (six to eight quads per year), with a survey line spacing of 500 meters in open basins, more dense on the flanks of mudbanks. GPS and bathymetry soundings are taken from a boat with a 25 cm draft. Data are collected on a quad-by-quad basis. The data are processed on a PC. Collection will begin in the eastern Bay and proceed westward.

Process_Date: not complete

Process_Comments and suggestions? Contact:

Contact_Information:

Contact_Person_Primary:

Contact_Person: Mark Hansen

Contact_Organization: US Geological Survey

Contact_Position: Project chief

Contact_Address:

Address_Type: mailing address

Address: 600 Fourth Street South

City: St. Petersburg

State_or_Province: FL

Postal_Code: 33701

Contact_Voice_Telephone: 727 893 3100 ext 3036

Contact_Facsimile_Telephone: 727 893 3333
Contact_Electronic_Mail_Address: mhansen@usgs.gov

Distribution_Information:

Distributor:

Contact_Information:

Contact_Person_Primary:

Contact_Person: Mark Hansen

Contact_Organization: US Geological Survey

Contact_Position: Project chief

Contact_Address:

Address_Type: mailing address

Address: 600 Fourth Street South

City: St. Petersburg

State_or_Province: FL

Postal_Code: 33701

Contact_Voice_Telephone: 727 893 3100 ext 3036

Contact_Facsimile_Telephone: 727 893 3333

Contact_Electronic_Mail_Address:

Hours_of_Service:

Resource_Description:

Distribution_Liability: The data have no explicit or implied guarantees.

Standard_Order_Process:

Digital_Form:

Digital_Transfer_Information:

Format_Name:

Digital_Transfer_Option:

Online_Option:

Computer_Contact_Information:

Network_Address:

Network_Resource_Name:

Fees:

Metadata_Reference_Information:

Metadata_Date: 19980916

Metadata_Comments and suggestions? Contact:

Contact_Information:

Contact_Person_Primary:

Contact_Person: Jo Anne Stapleton

Contact_Organization: US Geological Survey

Contact_Address:

Address_Type: mailing address

Address: 521 National Center

City: Reston

State_or_Province: VA

Postal_Code: 20192
Contact_Voice_Telephone: 703 648 4592
Contact_Facsimile_Telephone: 703 648 4614
Contact_Electronic_Mail_Address: jastapleton@usgs.gov
Metadata_Standard_Name: Content Standard for Digital Geospatial
Metadata
Metadata_Standard_Version: 19940608

Generated by mp on Wed Sep 16 15:05:04 1998
Raw data, metadata and maps are available upon request from
Mark Hanson; 600 4th Street South, St. Petersburg, Florida 33701; (727) 893-
3100 x3036; mhansen@wayback.er.usgs.gov